

# Two-dimensional self-modulation of lower hybrid waves in inhomogeneous plasmas

G. P. Leclert,<sup>a)</sup> Charles F. F. Karney,<sup>b)</sup> A. Bers,<sup>c)</sup> and D. J. Kaup<sup>d)</sup>

*Research Laboratory of Electronics and Plasma Fusion Center, Massachusetts Institute of Technology, Cambridge, Massachusetts 02139*

(Received 6 September 1977; final manuscript received 27 March 1979)

For lower hybrid waves in an inhomogeneous plasma, the two-dimensional self-modulation effects due to ponderomotive force are studied under the assumption that the field is electrostatic and has a narrow  $k$  spectrum. For a locally linear temperature profile and a broad class of density profiles, exact nonlinear solutions (solitons) are obtained by the inverse scattering method. The solitons decay and spread as they propagate. In addition to the usual area condition on the potential  $\int \phi d\xi \geq \pi/2$ , inhomogeneity introduces a second condition for solitons to occur. It is shown that this second condition is not satisfied in typical tokamak plasmas, i.e., there is no soliton formation, in contrast to the homogeneous case. Furthermore, the scaling of the threshold conditions with density and temperature makes them more difficult to satisfy in larger machines.

## I. INTRODUCTION

In the past few years there has been increasing interest in the lower hybrid resonance heating of tokamak plasmas. As in any heating scheme, one major problem is to insure that the incident power reaches the inner region of the plasma. In the linear regime, this gives an accessibility criterion<sup>1</sup> and conditions on the launching structure.<sup>2</sup> Furthermore, nonlinear phenomena can take place affecting the mode itself by either parametric excitations<sup>3</sup> or self-modulation. Here, we concern ourselves only with the last of these.

As the wave propagates toward the center of the plasma it encounters roughly three regions (Fig. 1): First, there is a low-density, inhomogeneous, cold plasma near the wall; here, a description of the plasma with the full set of electromagnetic equations is required (region I). Beyond the slow-wave cutoff, there is an inhomogeneous, warm plasma region (region II). Finally, near the center, the hot plasma is quasi-homogeneous (region III). In regions II and III the lower hybrid wave is essentially electrostatic. For a homogeneous plasma (such as region III), using the electrostatic approximation, Morales and Lee<sup>4</sup> have shown that the competition between the dispersive effects and the nonlinear perturbation due to the ponderomotive force can produce filamentation described by a modified Korteweg-de Vries equation. The onset of filamentation corresponds to the threshold for soliton solutions to the modified Korteweg-de Vries equation. In obtaining this result the authors rely upon the assumption that the solution for the potential remains real everywhere; however, the condition that power must flow into the plasma in a single resonance cone requires that the

potential be complex and the solution of a "complex modified Korteweg-de Vries" equation is required.<sup>5</sup> Unfortunately, general solutions of this equation are not known. However, the parallel (to  $B$ ) spectrum of waves launched at the wall from an appropriately phased array of waveguides, or slow-wave structure, is limited both from below (by accessibility and penetration-considerations) and from above (by electron Landau damping). Thus, the fields that penetrate the plasma have a relatively confined spectrum of wavenumbers. Under these conditions, a quasi-monochromatic description of the fields is appropriate. The wave envelope then obeys a nonlinear Schrödinger equation which predicts self-modulation if the following condition is fulfilled<sup>6</sup>:

$$\int_{-\infty}^{\infty} \frac{1}{\delta} \left( \frac{\frac{1}{4} \epsilon_0 |E_z(x=0)|^2}{nT} \right)^{1/2} \frac{dz}{\lambda_{De}} \geq \frac{\pi}{2}, \quad (1)$$

where  $z$  is the direction of the applied magnetic field,  $E_z(x=0)$  is the  $z$  component of the initial electric field,  $\lambda_{De}$  is the electron Debye length, and

$$\delta = 3\sqrt{2} \left[ 1 - \frac{1}{3} (\omega_{pe}/\Omega_e)^2 + \frac{1}{3} (\omega_{pe}/\Omega_e)^4 + (T_i/T_e) (\omega_{pi}/\omega)^4 \right]^{1/2}.$$

If one uses this condition locally for an inhomogeneous plasma (region II) by scaling down the density and temperature one finds that for typical tokamak plasmas and rf power levels, solitons can form only far from the center of the plasma. It follows that an analysis including inhomogeneity is necessary to obtain the criteria of formation and evolution of solitons. This is the aim of the present work. We find that the effect of inhomogeneity is indeed important, for it substantially increases the threshold at which solitons (that is, self-focusing and/or filamentation) can occur; furthermore, the solitons decay and spread as they propagate.

The analysis is carried out under the assumption of a narrow spectrum and within the electrostatic approximation. Section II gives the basic assumptions and equations of the model. Section III presents the restriction to narrow spectra and to a particular class of density and temperature profiles which lead (Sec. V) to an envelope equation in the form of a nonlinear Schrö-

<sup>a)</sup>Permanent address: Laboratoire de Physique des Milieux Ionisés, Université de Nancy, 54037 Nancy, France.

<sup>b)</sup>Present address: Plasma Physics Laboratory, Princeton University, Princeton, N. J. 08544.

<sup>c)</sup>Also Department of Electrical Engineering and Computer Science, Massachusetts Institute of Technology, Cambridge, Mass. 02139.

<sup>d)</sup>Permanent address: Department of Physics, Clarkson College of Technology, Potsdam, N. Y. 13676.

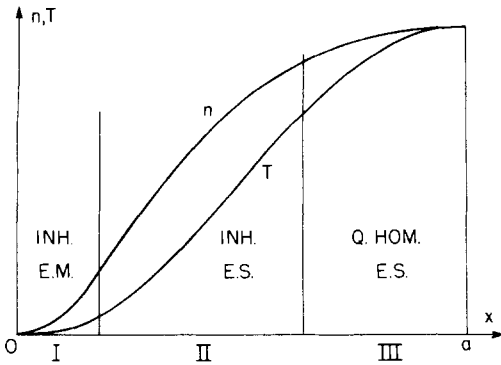


FIG. 1. Propagation of the lower hybrid wave in an inhomogeneous plasma, and range of validity of electrostatic and homogeneous approximations. The labels stand for: Q.HOM., quasi-homogeneous; INH., inhomogeneous; E.S., electrostatic; E.M., electromagnetic.

dinger equation in a transformed space. This allows us to obtain analytic expressions for the threshold and for the decaying solitons. In Sec. V we discuss the problem of the nonsoliton part of the solution (the "radiation") and the scaling of the threshold conditions. In particular, it turns out that this model does not predict soliton formation in both present day and future tokamak plasmas.

## II. BASIC EQUATIONS

We consider an inhomogeneous plasma in a uniform magnetic field  $B_0$ . The magnetic field is along  $z$  and the density and temperature vary in the  $x$  direction. The initial electric field is along  $z$  and the extent of the launching structure in the  $z$  direction is  $L$  (Fig. 2). We shall consider only two-dimensional effects, that is, we assume there is no variation along  $y$ . The source has an infinite extent in the  $y$  direction. Therefore, it is easy to see that there is no contribution from the  $\mathbf{E} \times \mathbf{B}$  term in the ponderomotive force.

We further assume that the lower hybrid wave is electrostatic. This is valid beyond a given position  $x$  where  $\omega_{pe}(x) \gg \omega$ , where  $\omega$  is the wave frequency and  $\omega_{pe}(x)$  is the local plasma frequency. Therefore, we neglect the phenomena that could take place near the plasma edge (i.e., we exclude region I of Fig. 1). Furthermore, the wave frequency is assumed to be near but greater than the lower hybrid frequency at the

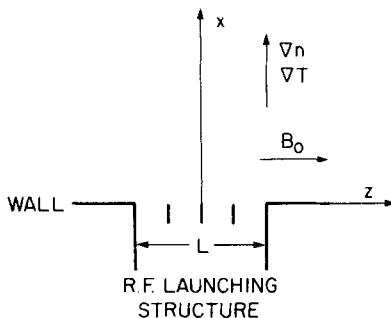


FIG. 2. Two-dimensional geometry of the model.  $L$  is the width of the incident field along the magnetic field.

center, so that the temperature effects give only small corrections to the cold plasma dispersion relation. The equation describing the lower hybrid potential  $\phi(x, z)$  in the linear regime is then given by (Appendix):

$$\partial_x K_{\perp} \partial_x \phi + \partial_x K_{\parallel} \partial_z \phi + \alpha \partial_x^4 \phi + \beta \partial_x^2 \partial_z^2 \phi + \gamma \partial_z^4 \phi + A \phi + B \partial_z^2 \phi = 0, \quad (2)$$

where

$$A \phi = \alpha(3L_N^{-1} + 2L_T^{-1}) \partial_x^3 \phi + [\alpha_{xx} + 2(\alpha L_N^{-1})_x] \partial_x^2 \phi + (\alpha L_N^{-1})_{xx} \partial_x \phi,$$

$$B \partial_z^2 \phi = \beta(\frac{3}{2}L_N^{-1} + L_T^{-1}) \partial_x \partial_z^2 \phi + \frac{1}{2} \beta_{xx} \partial_z^2 \phi,$$

$$K_{\perp} = 1 + \omega_{pe}^2 / \Omega_e^2 - \omega_{pi}^2 / \omega^2, \quad K_{\parallel} = 1 - \omega_{pe}^2 / \omega^2 - \omega_{pi}^2 / \omega^2,$$

$$\alpha = \frac{3}{4} \frac{v_e^2 \omega_{pe}^2}{\Omega_e^2 \omega^2} + 3 \frac{v_i^2 \omega_{pi}^2}{\omega^2 \omega^2},$$

$$\beta = - \frac{v_e^2 \omega_{pe}^2}{\Omega_e^2 \omega^2} + 6 \frac{v_i^2 \omega_{pi}^2}{\omega^2 \omega^2},$$

$$\gamma = 3 \frac{v_e^2 \omega_{pe}^2}{\omega^2 \omega^2} + 3 \frac{v_i^2 \omega_{pi}^2}{\omega^2 \omega^2},$$

$$v_j^2 = \frac{T_j}{m_j}, \quad L_N^{-1} = \frac{1}{n} |\partial_x n|, \quad L_T^{-1} = \frac{1}{T} |\partial_x T|.$$

The ponderomotive force of the lower hybrid wave produces a nonlinear density perturbation which modifies the density-dependent terms of Eq. (2). This density perturbation is given by<sup>4</sup>

$$\delta n / n = -\frac{1}{4} \epsilon_0 |\nabla \phi|^2 / (nT), \quad T = T_e + T_i. \quad (3)$$

Substituting (3) into (2) and neglecting the nonlinear modification of the thermal terms, we obtain the equation for  $\phi$  in the weakly nonlinear and inhomogeneous regime

$$K_{\perp} \partial_x^2 \phi + K_{\parallel} \partial_z^2 \phi + \alpha \partial_x^4 \phi + \beta \partial_x^2 \partial_z^2 \phi + \gamma \partial_z^4 \phi + A \phi + B \partial_z^2 \phi + (\partial_x K_{\perp}) \partial_x \phi + \frac{\epsilon_0}{4} [(1 - K_{\perp}) \partial_x \frac{|\nabla \phi|^2}{nT} \partial_x \phi + (1 - K_{\parallel}) \partial_z \frac{|\nabla \phi|^2}{nT} \partial_z \phi] = 0. \quad (4)$$

## III. CASE OF A NARROWBAND EXCITATION

In a lower hybrid heating experiment, the useful range of refractive indices is limited. The  $n_x$ 's smaller than the accessibility value (greater than 1) correspond to a part of the spectrum that does not penetrate into the plasma. On the other hand, large  $n_x$ 's (typically  $n_x > 10$ ) lead to strong Landau damping at the edge of the plasma. The actual width of the spectrum depends on the launching structure. For an array of four waveguides or more we can assume, in a first approximation, that the spectrum is of a narrow width centered around a given wavenumber  $k_x$ . The potential  $\phi$  can then be written in the form of a quasi-monochromatic plane wave

$$\phi(x, z) = \psi(x, z) \exp(ik_x z - i \int k_x dx), \quad (5)$$

where the envelope  $\psi(x, z)$  is slowly varying compared with  $k_x$  and  $k_x(x)$ . Since we wish to treat the inhomogeneous and nonlinear terms in (4) as a perturbation, we need only consider the leading order contributions

to these terms. Thus, we can simplify these terms by replacing  $\partial_x$  and  $\partial_z$  by  $-ik_x$  and  $ik_z$ , respectively. We next reduce the complexity of the remaining linear terms. We do this by treating dispersion as a weak perturbation of the same order as the effect of nonlinear terms. Neglecting dispersion entirely, the solution of  $\psi$  is

$$\psi(x, z) = \psi(z - \int g dx),$$

where  $g$  will be defined, i.e., the wave travels along characteristics. We will treat the effects of both nonlinearity and dispersion by letting  $\psi$  have an explicit  $x$  dependence; thus,

$$\phi(x, z) = \psi(\xi, x) \exp(ik_x z - i \int k_x dx), \quad (6)$$

where  $\xi = z - \int g dx$ . We assume the dependencies in (6) are ordered as follows<sup>6</sup>:

$$|ik_x| \gg |g\partial\xi| \gg |\partial_x|; \quad |ik_z| \gg |\partial_z|.$$

Substituting (6) into (4) we see that the lowest order and next to lowest order contributions vanish if we take

$$D(k_x, k_z) = -k_x^2 K_1 - k_z^2 K_2 + \alpha k_x^4 + \beta k_x^2 k_z^2 + \gamma k_z^4 = 0, \quad (7)$$

$$g = - \frac{\partial D / \partial k_z}{\partial D / \partial k_x} \approx \left( - \frac{K_2}{K_1} \right)^{1/2}. \quad (8)$$

The next order terms give the equation for  $\psi$ :

$$i\psi_x + \frac{1}{2}g' \psi_{xx} + \frac{\epsilon_0 k_x^3}{8K_1 n T} |\psi|^2 \psi + \frac{i}{2} \left[ \frac{\partial_x (k_x K_1)}{k_x K_1} - \frac{k_x^2}{K_1} (3L_N^{-1} + 2L_T^{-1})\alpha - \frac{k_x^2}{K_1} (\frac{3}{2}L_N^{-1} + L_T^{-1})\beta g^{-2} \right] \psi = 0, \quad (9)$$

where we have defined

$$g' = \frac{dg}{dk_x} = 3 \frac{k_x^3}{k_x^2 K_1} (\alpha + \beta g^{-2} + \gamma g^{-4}). \quad (10)$$

The three terms in the brackets of Eq. (9) represent the effect of inhomogeneity. We shall use our model in the density gradient, region II of Fig. 1, where the density and temperature are well below their maximum (center) values. Then, the first term in the brackets (which comes from the cold plasma part of the dispersion relation) is much greater, by a factor of the order  $(k_x \lambda_{De})^{-2}$ , than the other two (which come from the small thermal part). Hence, we keep only the first term. We then transform to the dimensionless variables

$$q = \psi/V, \quad V^2 = 8nTK_1 g' / \epsilon_0 k_x^3 L^2, \quad (11)$$

$$\tau = (1/2L^2) \int g' dx, \quad \xi = \xi/L,$$

where  $L$  is given in Fig. 2. We note that

$$|q|^2 = \frac{\frac{1}{4}\epsilon_0 |E_x|^2 L^2}{18nT \lambda_{De}^2}$$

is related to the energy density measure that enters into the soliton formation threshold condition for a homogeneous plasma, viz, Eq. (1). The function  $q$  obeys the equation

$$iq_\tau + q_{\xi\xi} + 2|q|^2 q + if(\tau)q = 0, \quad (12)$$

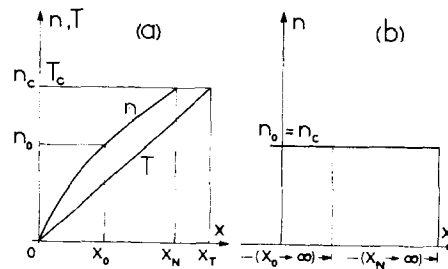


FIG. 3. Density and temperature profiles. (a) Model profiles for the density and temperature [Eq. (15)];  $x_0$  is the distance between the origin and the initial condition. (b) Limit of a homogeneous plasma,  $x_0, x_N, x_T \rightarrow \infty$ .

where

$$f(\tau) = \frac{1}{2} \partial_\tau \ln(K_1 k_x V^2). \quad (13)$$

From (12) one can easily derive the relation

$$F(\tau) \int_{-\infty}^{\infty} |q|^2 d\xi = \text{const}, \quad (14)$$

where  $F(\tau) = \exp[\int \tau 2f(\tau) d\tau] = K_1 k_x V^2$ . It is easily verified that (14) is the law of conservation of energy.<sup>7</sup> The linear dispersionless solution of Eq. (12) shows that  $f(\tau)$  represents the WKB effect

$$q(\tau) = q(0) \exp \left[ \int f(\tau) d\tau \right] = q(0) (K_1 k_x)^{-1/2} V(\tau),$$

or

$$\psi(\tau)/\psi(0) = (K_1 k_x)^{-1/2}.$$

To proceed further we model the profiles in the region of interest (region II of Fig. 1) by the expressions

$$n = n_c (x/x_N)^r, \quad T = T_c (x/x_T)^r, \quad (15)$$

where  $n_c, T_c$  are the values at the center and  $r, x_N,$  and  $x_T$  are locally adjustable parameters for fitting the density and temperature profiles. (These quantities may be very different from the local gradient lengths  $L_N$  and  $L_T$ ). Note that we restrict the analysis to a temperature profile increasing linearly; this should not constitute a serious limitation. More important, by choosing  $r \neq 1$  the density and temperature gradients can be made locally different ( $L_N \neq L_T$ ), in agreement with experimental data.<sup>8</sup>

Obviously, we cannot take the initial condition at a point arbitrarily close to  $x=0$ . Because of the electrostatic assumption, the density at the initial condition must be high enough so that the local plasma frequency

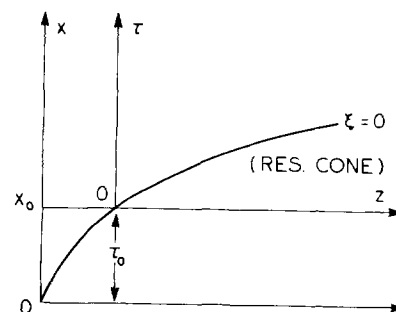


FIG. 4. Coordinate transformation, Eq. (11); the initial condition is taken at the point  $x_0$  corresponding to  $\tau=0$ .

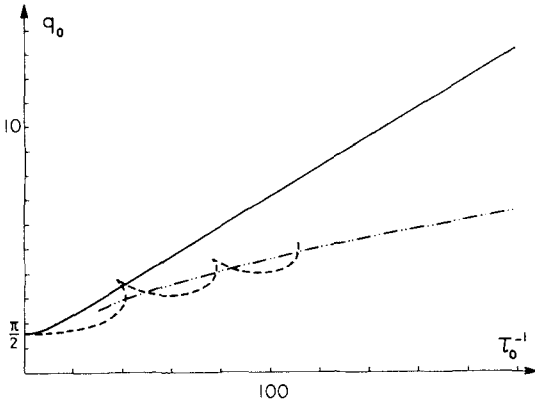


FIG. 5. Threshold curves for soliton formation in field envelopes of different shapes.  $q_0$  is the amplitude of the normalized potential and  $\tau_0^{-1}$  is a measure of the inhomogeneity. Gaussian: (—). Square: (-----) and (- · - · - ·); the last curve represents the approximate expression, Eq. (20c), valid at large inhomogeneity.

$[n_0 e^2 / (\epsilon_0 m_e)]^{1/2} \gg \omega$ . From Eq. (15), it immediately follows that the abscissa of this point  $x_0$  is given by  $(x_0/x_N) = (n_0/n_c)$ . Therefore,  $x_0$  is related to the density gradient. For a given  $r$ , the smaller the gradient (the greater  $x_N$ ), the greater the value of  $x_0$ . Keeping  $r$  fixed we may go to the limit of a homogeneous plasma [ $n(x) = n_c$ ,  $T(x) = T_c$ ] by letting  $x_N, x_T, x_0 \rightarrow \infty$ , with  $x/x_N, x/x_T \rightarrow 1$  (Fig. 3).

We then transform from  $x$  to  $\tau$  in such a way that  $\tau = 0$  at  $x = x_0$ . Again, we use the fact that in the density gradient, region II of Fig. 1, the density and temperature are well below their maximum (center) values. The wave frequency is greater than the lower hybrid frequency at the center. Furthermore, we assume that the electron gyrofrequency and the plasma frequency at the center are comparable. Therefore, we may make the following approximations ( $\omega_{pe}^2 \ll \Omega_e^2$ ,  $\omega_{pi}^2 \ll \omega^2$ ):

$$K_1 \approx \text{const} \approx 1, \\ \alpha + \beta g^{-2} + \gamma g^{-4} = 3\lambda_{De}^2 [1 + O(\omega_{pe}^2/\Omega_e^2)] \approx 3\lambda_{De}^2.$$

We then obtain

$$f(\tau) = \frac{1}{2(\tau + \tau_0)}. \quad (16)$$

Here,  $\tau_0$  corresponds to the change of origin (Fig. 4)

$$\tau_0 = \int_0^x \left[ \frac{g'(x)}{(2L^2)} \right] dx = \frac{9}{r+4} \left( \frac{k_x^3 \lambda_{De}^2}{k_z^2 K_1 L^2} \right) x_0.$$

The homogeneous plasma ( $x_0 \rightarrow \infty$ ) corresponds to the limit  $\tau_0 \rightarrow \infty$  which indeed makes  $f(\tau)$  zero.

#### IV. SOLUTION OF THE NONLINEAR ENVELOPE EQUATION

With the previous choice of a linearly increasing temperature profile the envelope Equation (12) becomes

$$iq_\tau + q_{\xi\xi} + 2|q|^2 q + \frac{i}{2(\tau + \tau_0)} q = 0. \quad (17)$$

Let us define the transformation:

$$\theta = \tau / (1 + \tau/\tau_0), \\ \sigma = \xi / (1 + \tau/\tau_0), \quad (18) \\ q(\tau, \xi) = \frac{1}{1 + \tau/\tau_0} w(\tau, \xi) \exp\left(\frac{i\xi^2}{4(\tau + \tau_0)}\right).$$

It then follows that  $w(\theta, \sigma)$  satisfies the usual nonlinear Schrödinger equation

$$iw_\theta + w_{\sigma\sigma} + 2|w|^2 w = 0 \quad (19a)$$

with the initial condition:

$$w(0, \sigma) = q(0, \sigma) \exp[-i(\sigma^2/4\tau_0)]. \quad (19b)$$

The homogeneous case is recovered by taking the limit  $\tau_0 \rightarrow \infty$ , and leads to the threshold condition (1). For a finite value of  $\tau_0$  the initial condition is complex, and as we shall see, this greatly increases the threshold for soliton formation, i.e., for such phenomena as filamentation or self-focusing of the resonance cone.

#### A. Threshold conditions for solitons

Equations (19) have soliton solutions if the associated eigenvalue problem<sup>9</sup>:

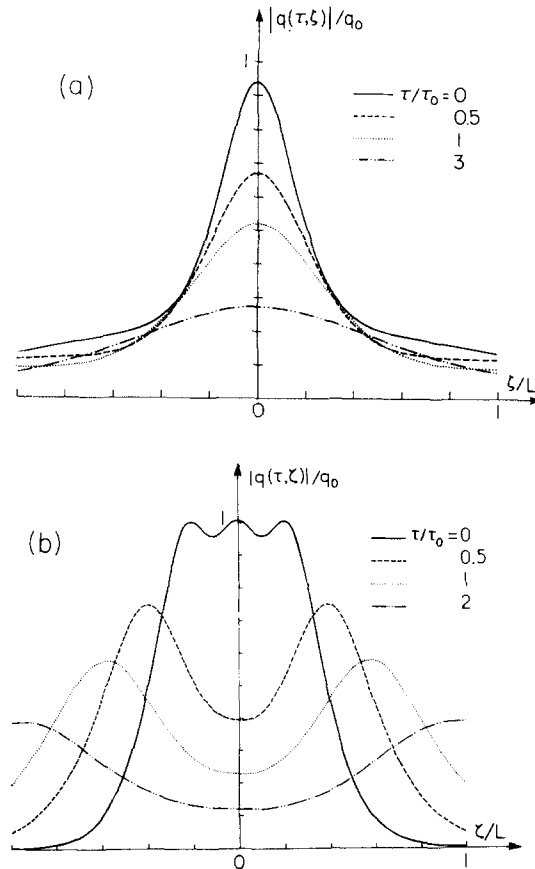


FIG. 6. Soliton part of the solution of the nonlinear envelope Eq. (17), when  $q_0 = 7$  and  $\tau_0 = 1/49$ . (a) Gaussian initial envelope, there are two imaginary eigenvalues  $\lambda_1 = 0.5i, \lambda_2 = 0.1i$ . (b) Square initial envelope, the two eigenvalues are complex,  $\lambda_1 = 0.3 + 0.6i, \lambda_2 = -0.3 + 0.6i$ . The resonance cone is at  $\xi = 0$ .

$$(\partial_\sigma + i\lambda)h_1(\sigma) = q(0, \sigma)\exp[-i(\sigma^2/4\tau_0)]h_2(\sigma),$$

$$(\partial_\sigma - i\lambda)h_2(\sigma) = -q^*(0, \sigma)\exp[i(\sigma^2/4\tau_0)]h_1(\sigma),$$

has eigenvalues  $\lambda$  in the upper-half plane,  $\text{Im } \lambda > 0$ . Such a set of equations has been solved in the context of the three-wave interaction problem when  $q(0, \sigma)$  is either a square pulse<sup>10</sup> or a Gaussian pulse.<sup>11</sup> We use these results to display in Fig. 5 the behavior of the threshold for soliton formation for the square  $q(0, \sigma) = q_0$ ,  $|\sigma| \leq 1/2$ , and for the Gaussian  $q(0, \sigma) = q_0 \exp(-\pi\sigma^2)$ . With this choice,  $\int q(0, \sigma) d\sigma = q_0$  for both cases. The threshold for the Gaussian increases linearly with  $\tau_0^{-1}$ . Therefore, at large inhomogeneity it becomes much higher than the threshold for the square which behaves like  $\tau_0^{-1/2}$ : For initial conditions with smooth boundaries, the dephasing along the boundaries produced by inhomogeneity makes soliton formation more difficult. The structure of the threshold for the square is due to the occurrence of eigenfunctions tied to the sharp boundaries.<sup>10</sup> When the inhomogeneity increases, these eigenmodes become more and more highly localized; thus, in an actual experiment, it is unlikely that these modes could form and the actual threshold would be somewhat higher. At large inhomogeneity the thresholds can be expressed as:

$$q_0 \geq \pi/2 \quad (\text{both cases}), \quad (20a)$$

$$q_0 \tau_0 \geq 0.1 \quad (\text{Gaussian}), \quad (20b)$$

$$q_0^2 \tau_0 \geq 0.2 \quad (\text{square}). \quad (20c)$$

Condition (20a) is the same as in the homogeneous case. Inhomogeneity causes the occurrence of the second condition (20b) or (20c). In terms of the physical parameters Eqs. (20) become

$$q_0^2 = \frac{1}{18} \frac{\frac{1}{2} \epsilon_0 |E_{s0}|^2 L^2}{n_0 T_0 \lambda_{De}^2} \geq \frac{\pi^2}{4}, \quad (21a)$$

$$q_0^2 \tau_0 = \frac{1}{r+4} \frac{e^3}{8 \epsilon_0^{1/2} m_e^{3/2} c \omega^2 x_0} \frac{n_s}{T_0} \frac{n_0^{1/2}}{T_0} |E_{s0}|^2 \geq 0.2 \quad (\text{square}), \quad (21b)$$

$$q_0^2 \tau_0^2 = \frac{9}{8(\gamma+4)^2} \frac{e^4}{\epsilon_0 m_e^3 c^2 \omega^4} \frac{n_s^2 T_{e0}}{T_0} n_0 \frac{x_0^2}{L^2} \times |E_{s0}|^2 \geq 10^{-2} \quad (\text{Gaussian}). \quad (21c)$$

The subscript 0 stands for all variables evaluated at the point  $x_0$ . We shall later discuss the scaling and numerical values of these expressions.

## B. Soliton solutions

If the conditions (20) are fulfilled, the general solution of the envelope equation (19a) is composed of one or more solitons and of a nonsoliton part, the radiation. Since soliton formation is characteristic of strong nonlinear effects, in this section we focus on the soliton part and illustrate the nonlinear behavior of the lower hybrid envelope with the one and two-soliton solutions.

If there is only one soliton corresponding to the eigenvalue  $\lambda$ ,  $\lambda = i\eta$  ( $\eta$  real), the normalized potential  $q$  is expressed as

$$q(\tau, \xi) = 2 \frac{\eta}{1 + \tau/\tau_0} \text{sech} \left( \frac{2\eta}{1 + \tau/\tau_0} \xi \right) \times \exp \left[ i \left( \frac{4\eta^2 \tau}{1 + \tau/\tau_0} + \frac{1}{4(\tau + \tau_0)} \xi^2 \right) \right]. \quad (22)$$

Rewriting the transformation (11) as

$$\frac{\psi}{\psi_0} = \frac{q}{q_0} \frac{x}{x_0}; \quad \frac{1}{1 + \tau/\tau_0} = \left( \frac{x_0}{x} \right)^{2+r/2}$$

one easily obtains the unnormalized potential  $\psi(x, \xi)$ ; for example,

$$\frac{|\psi|}{|\psi_0|} = 2 \frac{\eta}{q_0} \left( \frac{x_0}{x} \right)^{1+r/2} \text{sech} \left[ 2\eta \frac{\xi}{L} \left( \frac{x_0}{x} \right)^{2+r/2} \right]. \quad (23)$$

This last equation shows that the soliton decays and spreads with a characteristic length of the order of  $x_0$ . The steeper the density gradient (i.e., the larger the exponent  $r$ ), the faster the decay. Note that  $|\psi|$  has its maximum for  $\xi = 0$ ; that is, the soliton stays in the resonance cone. In general  $[\text{Re}(\lambda) \neq 0]$ , the soliton moves out of the resonance cone.

It is worth examining (22) in some detail since it illustrates the transformation used to derive the nonlinear Schrödinger equation (18). From (22) we have

$$(\tau + \tau_0) \int |q|^2 d\xi = \text{const}, \quad \int |q| d\xi = \pi.$$

The first of these relations follows from the energy conservation law, (14). It shows that as the pulse propagates into the plasma, its "squared area" decreases (due to WKB effects). The second relation which is true for solitons of the homogeneous nonlinear Schrödinger equation [(17) with the last term omitted] states that the "absolute area" of a soliton is constant. These constraints can only be reconciled if the soliton spreads out as it propagates. This spreading is caused in (22) by the quadratic, chirping, term in the phase. This gives the right and left sides of the pulse outwardly directed group velocities, which leads to the spreading. Thus, (18) provides the chirping factor in the transformation from  $w$  to  $q$  and the spreading out in the transformation from  $\sigma$  to  $\xi$ . The transformation from  $\theta$  to  $\tau$  reflects the fact that as the pulse spreads out and decays the time scale in which solitons interact becomes larger, until at  $\theta = \tau_0$ , the time scale is infinite.

We now see the origin of the increased soliton thresholds of Sec. IVA. The inhomogeneity means that the solitons are chirped. We could have avoided the additional conditions on soliton formation, (21b) and (21c), had we chosen correctly chirped initial conditions. Such initial conditions are unlikely to occur in practice. Thus, the additional threshold conditions are a result of our wishing to use initial pulses  $q(0, \xi)$ , which have no phase variation, and which as a result do not readily decompose into chirped solitons. (Note, therefore, that the increased threshold is not a consequence of the soliton propagating into a region of lower nonlinearity. Indeed, we obtain the same thresholds if we reverse  $\tau$ , and allow the solitons to propagate into a region of increased nonlinearity).

Although the expressions become complicated once

several solitons are present, they exhibit the same qualitative behavior. Figure 6 displays the soliton part of the solution for the case  $q_0 = 7$  and  $\tau_0 = 1/49$ ; two solitons are present in the initial condition which is either a Gaussian [Fig. 6(a)] or a square [Fig. 6(b)]. In the former case the two solitons form a bound state and do not separate; they stay in the resonance cone. In the latter case the two solitons separate and leave the resonance cone, i.e., filamentation occurs. (However, one should note that, in general, this filamentation will only occur *initially*, up until  $\tau \gtrsim \tau_0$ . For  $\tau \gg \tau_0$ ,  $\theta$  as defined by Eq. (18) has essentially reached its asymptotic value of  $\tau_0$ , and thereafter no further separation in the filaments will occur.) In our model it turns out that this behavior is due to the fact that the eigenvalues are always purely imaginary for the Gaussian and can be complex for the square.<sup>12</sup> From these results we conclude that soliton formation in an inhomogeneous plasma leads to a fast broadening of the linear resonance cones and a transport of part of the energy away from these resonance cones. One should note that due to the presence of radiation these solutions are only approximate; this is particularly apparent in the case of the square. Numerical solutions of (17) by Pereira<sup>13</sup> with initial conditions and the parameter  $\tau_0 = 1/49$  of Fig. 6 corroborate our conclusions. The initial Gaussian profile decreases in amplitude and widens as shown in Fig. 6(a). The numerical solutions with the square initial condition initially develop similarly to Fig. 6(b); however, at long times the computation shows a central repeaking. This is due to the fact that the radiation eventually dominates the solution. We shall say more about this in Sec. VB.

## V. DISCUSSION

### A. Solitons versus radiation

In the  $(\theta, \sigma)$  space, the solution consists of solitons of constant amplitude and of a certain amount of radiation. One usually neglects the radiation because it spreads out asymptotically ( $\theta \rightarrow \infty$ ). However, in transformation (18)  $\theta$  goes from 0 to  $\tau_0$  when  $\tau$  goes from 0 to  $\infty$ . Therefore, one has to know the importance of the radiation for  $\theta \leq \tau_0$ . We discuss this problem on the basis of qualitative arguments.

In order for solitons to play an important role the following two conditions must be fulfilled:

(i) The radiation part must be initially small, that is, the initial condition can be approximated by a  $N$ -soliton formula. This can be done only if the quadratic phase factor in (19b) is small enough.

(ii) The radiation must stay negligible for all times. The behavior of the radiation is essentially linear in nature, so we look at the linear solution  $w_1$  of Eq. (19a) which can be obtained by standard techniques [we assume a Gaussian initial condition,  $q(0, \sigma) = w_0 \exp(-4\sigma^2)$ ]:

$$|w_1|^2 = w_0^2 \frac{\tau_0}{[256\tau_0^2\theta^2 + (\tau_0 - \theta)^2]^{1/2}},$$

where  $w_0$  is the measure of the initial radiation part. When  $\theta$  goes from 0 to  $\tau_0$ ,  $|w_1|^2$  initially grows and

reaches its maximum value

$$|w_1|_{\max}^2 = w_0^2 \frac{(256\tau_0^2 + 1)^{1/2}}{16\tau_0} \quad (24)$$

at the point

$$\theta_{\max} = \frac{\tau_0}{1 + 256\tau_0^2} < \tau_0.$$

This unusual behavior is due to the fact that the initial condition (19b) for  $w(0, \sigma)$  consists of radiation whose waves have initial velocities directed toward the initial disturbance, causing it to grow initially. This focusing is an artifact of the transformation, (18). If we look at the behavior of  $q$  in the linear equation, we find that it always decays for these conditions. We choose to examine the behavior of the radiation using  $w$ , since then comparison with the soliton is facilitated, the soliton having constant amplitude in  $w$ .

From Eqs. (19b) for the initial condition and (24) for the radiation we see that both conditions can be achieved if the quantity  $(16\tau_0)^{-1}$  is smaller than a few units, say  $\pi$  (which gives a dephasing of  $2\pi$  across the width of the initial condition). Therefore, the condition

$$\tau_0 \geq 1/16\pi \quad (25)$$

means that solitons (if any) play an important role in the evolution of the envelope (Fig. 7). If  $\tau_0$  is too small, the threshold is very high, and the energy associated with the soliton part becomes negligible compared with the energy of the radiation part. Coming back to the case shown in Fig. 6, we see that condition (25) is marginally satisfied. Whether the radiation is important depends on the actual shape of the initial condition; for the square one can expect that the two-soliton solution is not very accurate.

From the analysis of both the solitons and the radiation, we can construct the following picture of what should happen when both solitons and radiation are present. When  $\tau_0$  is much larger than the limit given by

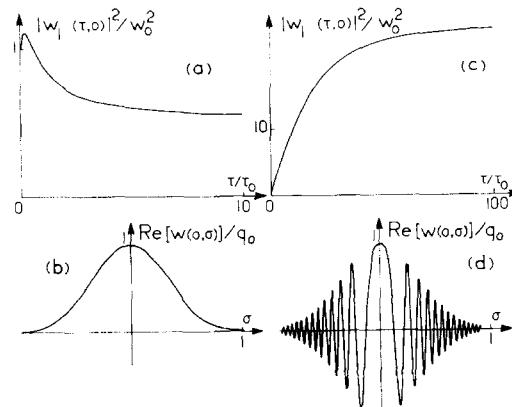


FIG. 7. Influence of the inhomogeneity parameter  $\tau_0$  on the radiation. The left part of the figure corresponds to weak inhomogeneity,  $\tau_0 = 1/8$ ; the right part, to strong inhomogeneity,  $\tau_0 = 2.5 \times 10^{-2}$ . The top curves represent the evolution of the "radiation"  $|w_1|$ . The bottom curves show the corresponding initial condition  $\text{Re}[w(0, \sigma)]$ . A strong inhomogeneity means a "chirped" initial condition and a growth of the radiation (in terms of the function  $w$ ).

Eq. (25), the solitons will probably have sufficient time to form filaments, while the swelling of the radiation will be minimal. For  $\tau_0$  on the order of the limit in Eq. (25), we can expect to see a significant swelling in the radiation around the value of  $\theta_{\max}$  given here, while due to the small value of  $\tau_0$ , the final net filamentation of the solitons should be minimal, although initially fast. (Also, we should point out that Pereira's numerical results<sup>13</sup> show that at least in some cases, this swelling of the radiation can dominate and swamp the soliton structure.) For  $\tau_0$  smaller than the limit in (25), the solitons will not have time even to move initially, while the radiation will quickly swell and dominate, as shown in Fig. 7(c). Finally, whenever  $\tau \gg \tau_0$  the solution to (19a) will asymptotically approach  $w(\tau_0, \xi\tau_0/\tau)$ , since  $\theta$  will asymptotically approach  $\tau_0$ . The total solution of (17) is then

$$q(\xi, \tau) = (\tau_0/\tau)w(\tau_0, \xi\tau_0/\tau)\exp(\frac{1}{4}i\xi^2/\tau).$$

In this regime, the solution simply decays as  $\tau^{-1}$  and stretches out.

Since the radiation plays an important role in the solution for many initial conditions, a full analysis of (17) should include the effects of nonlinearity on the radiation. This would require applying and extending the results of Ref. 14.

## B. Scaling

We shall now express the threshold conditions in terms of quantities useful in a fusion experiment, like the rf and Ohmic powers and the machine parameters. Since the Gaussian has a higher threshold than the square, we only consider the latter which will give necessary conditions for soliton formation. Note that in a real experiment the threshold will certainly be higher (see Sec. IVA). Assuming perfect power coupling from an external source, we relate the field inside the plasma to the incident rf power<sup>15</sup>

$$|E_x|^2 \approx \frac{n_x}{\epsilon_0 c} \frac{\omega}{\omega_{ep}} \frac{P}{LH}, \quad (26)$$

where  $H$  is the height of the launching structure in the  $y$  direction (strictly speaking, since  $H$  should be infinite in our two-dimensional model,  $P/H$  is the power by unit of length in the  $y$  direction). For lower hybrid waves the wave frequency is of the order of the ion plasma frequency at the center. Thus, we get

$$0.12n_x \frac{PL}{H} \frac{1}{T_c T_{ec}} \left(\frac{x_T}{x_0}\right)^2 \left(\frac{x_N}{x_0}\right)^{r/2} \geq \frac{\pi^2}{4}, \quad (27a)$$

$$\frac{21}{4+r} 10^{-4} n_x^2 \frac{P}{LH} x_T \frac{1}{n_c^{1/2} T_c} \geq 0.2. \quad (27b)$$

In these expressions the density is in units of  $10^{14} \text{ cm}^{-3}$ , the temperature in keV and the power in MW.

So far,  $x_0$  is undetermined. If the launching structure can be put into the plasma  $x_0$  can be chosen arbitrarily and for low temperature, low density plasmas the conditions (27) can easily be satisfied together with the condition (25). Therefore, in such plasmas the propagation of lower hybrid resonance cones may be

subject to strong self-modulation phenomena.

For fusion plasmas, however, the rf wave is launched from outside and we shall evaluate the criteria with the smallest possible value of  $x_0$ . Let us define  $x_0$  as the point where the electrostatic assumption becomes valid; we choose the point where  $k_x = 10k_x$ . This gives  $x_0/x_N = 10^{2/r} (m_e/m_i)^{1/r}$ . We further introduce the Ohmic power  $P_O \approx 2\pi^2 R a^2 n_c T_c / \tau_E$ , where  $a$  and  $R$  are the minor and major radii of the torus and the energy confinement time  $\tau_E$  scales like  $\tau_E = 0.5 \times 10^{-20} n_c a^2$ .<sup>16</sup> In the same units as previously we have

$$1.3 \times 10^{5/(2r)} n_x \frac{LR}{H} \left(\frac{x_T}{x_N}\right)^2 \frac{P}{P_O} \frac{1}{T_{ec}} \geq 1, \quad (28a)$$

$$\frac{5}{4+r} 10^{-3} n_x^2 \frac{x_T R}{LH} \frac{P}{P_O} \frac{1}{n_c^{1/2}} \geq 1. \quad (28b)$$

The first condition is easily satisfied in any tokamak plasma. For example, if  $n_x = 5$ ,  $P/P_O = 1$ ,  $T_{ec} = 1 \text{ keV}$ ,  $R \approx 0.5 \text{ m}$ ,  $r = 1$ , and taking  $L$ ,  $H$ ,  $x_N$ , and  $x_T$  of the order of  $a \approx 0.1 \text{ m}$ , the left-hand-side of (28a) is  $10^3$ .

However, for  $n_c = 10^{14} \text{ cm}^{-3}$  and the previous values we find that the left-hand-side of (28b) is 0.1, i.e., the second condition is not satisfied by an order of magnitude. Notice that this condition, unlike the previous one, is almost independent of the actual density profile.

Furthermore, the scaling with density and temperature indicates that the requirements (28) are more difficult to meet in larger machines. Therefore, we conclude that in the limit of validity of the model, nonlinear effects on self-modulation cannot substantially affect the lower hybrid heating in present and future tokamak plasmas, because the necessary conditions are not even satisfied [we also note that even if there were solitons, they would carry very little energy, because here  $16\pi\tau_0 \ll 1$ , see condition (25)]. This result is essentially due to inhomogeneity: a homogeneous analysis would have given only the condition (28a) which predicts a large number of solitons.

Since self-focusing or filamentation is produced by the soliton part of the nonlinear Schrödinger equation and since solitons do not form, we conclude that, in the limit of validity of this model, such phenomena will not occur in a lower hybrid heating experiment.

## C. Limitations of the analysis

We have been able to obtain analytical expressions for the nonlinear evolution of the envelope and for the thresholds for soliton formation. This relies upon a few assumptions that we shall discuss briefly.

The need of a finite  $x_0$  where we define the initial condition results from the electrostatic approximation. We have assumed that the wave travels without modification from the external source to the point  $x_0$ . If drastic changes occur near the plasma edge, however, the envelope at  $x_0$  may be very different from a Gaussian. Similarly, Eq. (3) for the nonlinear density perturbation is no longer valid when  $\delta n/n$  becomes of the order of unity. (For tokamak parameters with our choice of  $x_0$

we always find  $\delta n/n < 10^{-2}$ .) These considerations and the results of the present analysis indicate that in order to have a complete understanding of selfmodulation, one has to study the nonlinear behavior of the lower hybrid wave near the edge (region I of Fig. 1). This must be done with the use of the full set of electromagnetic equations and a nonlinear equation allowing a proper transition from the plasma to the vacuum region.

The assumption of a narrow spectrum (which leads to the nonlinear Schrödinger equation) is only marginally valid for a four-waveguide array properly phased and powered and becomes questionable for one or two waveguides. Without this assumption, the nonlinear equation is a complex modified Korteweg-de Vries equation<sup>5</sup> with an additional term due to plasma inhomogeneity. Whether this equation has lower thresholds is an open question.

Finally, we note that three dimensional effects (finite  $k_y$  and  $\mathbf{E} \times \mathbf{B}$  coupling) have been shown to be important for the stability of lower hybrid solitons in a homogeneous plasma,<sup>17</sup> which have not been considered here.

## ACKNOWLEDGMENTS

We thank Dr. N. Pereira for useful discussion and for sending us his results on the numerical integration of Eq. (17). We also thank the referee for valuable comments and suggestions that helped to improve the presentation of our results.

This work was supported by the National Science Foundation (Grant ENG-75-06242 and MPS 75-07568), the U. S. Energy Research and Development Administration (Contract EX-76-01-22959), and the Office of Naval Research (Contract N00014-76-C-0867).

## APPENDIX: LINEAR EQUATION FOR THE LOWER HYBRID WAVE IN AN INHOMOGENEOUS PLASMA

We consider a two-fluid model with the electrostatic assumption. We assume there is no  $y$  dependence. The linearized equations for the density perturbation  $n_j$  and velocity  $\mathbf{v}_j$  due to the electric field  $\mathbf{E}$  of frequency  $\omega$  are

$$-i\omega n_j + \nabla \cdot (n_0 \mathbf{v}_j) = 0 \quad (\text{A1})$$

$$-i\omega \mathbf{v}_j = \frac{q_j}{m_j} (\mathbf{E} + \mathbf{v}_j \times \mathbf{B}_0) - \frac{1}{m_j n_0} \nabla (n_j T_j), \quad (\text{A2})$$

$n_0 = n_0(x)$  is the unperturbed density for both ions and electrons. The charge  $q_j = \epsilon_j e$  where  $\epsilon_j = \pm 1$ . Poisson equation is

$$\nabla \cdot \mathbf{E} = -\nabla^2 \phi = (e/\epsilon_0)(n_i - n_e). \quad (\text{A3})$$

In deriving (A1) and (A2) we have neglected the drift velocity due to the density and temperature gradients

$$\mathbf{v}_{j0} = (\epsilon_j/m_j n_0 \Omega_j) \partial_x (n_0 T_j) \hat{y}, \quad (\text{A4})$$

where  $\Omega_j$  is the gyrofrequency. One can see that this is justified if  $|\partial_x v_{j0}| \ll \Omega_j$ . This inequality is always satisfied in tokamak plasmas. Equation (A2) has the solution

$$\mathbf{v}_j = \mathbf{M}_j \cdot \mathbf{E} - (1/n_0 q_j) \mathbf{M}_j \cdot \nabla (n_j T_j), \quad (\text{A5})$$

where  $\mathbf{M}_j$  is the usual mobility tensor

$$\mathbf{M}_j = \frac{q_j}{m_j} \begin{bmatrix} \frac{i\omega}{\Omega_j^2 - \omega^2} & \frac{\Omega_j}{\Omega_j^2 - \omega^2} & 0 \\ \frac{-\Omega_j}{\Omega_j^2 - \omega^2} & \frac{i\omega}{\Omega_j^2 - \omega^2} & 0 \\ 0 & 0 & \frac{0}{i\omega} \end{bmatrix}. \quad (\text{A6})$$

Using (A5) in (A1) we obtain

$$n_j = \frac{1}{i\omega} \nabla \cdot n_0 \mathbf{M}_j \cdot [\mathbf{E} - \frac{1}{n_0 q_j} \nabla (n_j T_j)]. \quad (\text{A7})$$

The thermal terms are assumed to be only a small correction to the cold plasma results, so that we iterate (A7)

$$n_j = \frac{1}{i\omega} \nabla \cdot n_0 \mathbf{M}_j \cdot \mathbf{E} + \frac{1}{q_j \omega^2} \nabla \cdot \mathbf{M}_j \cdot \nabla T_j \nabla \cdot n_0 \mathbf{M}_j \cdot \mathbf{E}. \quad (\text{A8})$$

We can rewrite the Poisson equation as

$$\nabla \cdot \mathbf{K} \cdot \nabla \phi - \nabla \cdot \mathbf{Q} \cdot \nabla \phi = 0, \quad (\text{A9})$$

where  $\mathbf{K} = 1 + [ie/(\epsilon_0 \omega)] n_0 (\mathbf{M}_i - \mathbf{M}_e)$  is the cold plasma dielectric tensor and  $\mathbf{Q} = (1/\epsilon_0 \omega) (\mathbf{M}_e \cdot \nabla T_e \nabla \cdot n_0 \mathbf{M}_e + \mathbf{M}_i \cdot \nabla T_i \nabla \cdot n_0 \mathbf{M}_i)$  represents the thermal corrections in the presence of inhomogeneity. Equation (A9) is

$$\partial_x K_{\perp} \partial_x \phi + \partial_x K_{\parallel} \partial_x \phi + \alpha \partial_x^4 \phi + \beta \partial_x^2 \partial_x^2 \phi + \gamma \partial_x^4 \phi + A \phi + B \partial_x^2 \phi = 0. \quad (\text{A10})$$

In Eq. (A10) one has

$$\alpha = \frac{v_e^2 \omega_{pe}^2}{\Omega_e^2 \Omega_e^2} + \frac{v_i^2 \omega_{pi}^2}{\omega^2 \omega^2},$$

$$\beta = -\frac{v_e^2 \omega_{pe}^2}{\Omega_e^2 \omega^2} + \frac{v_i^2 \omega_{pi}^2}{\omega^2 \omega^2},$$

$$\gamma = \frac{v_e^2 \omega_{pe}^2}{\omega^2 \omega^2} + \frac{v_i^2 \omega_{pi}^2}{\omega^2 \omega^2}.$$

By replacing these expressions by the more accurate ones derived from kinetic theory<sup>18</sup> Eq. (A10) is Eq. (2). A slightly different expression has been derived by Sanuki and Ogino.<sup>19</sup>

<sup>1</sup>V. E. Golant, Zh. Tekh. Fiz. (U.S.S.R.) **41**, 2492 (1971) [Sov. Phys.-Tech. Phys. **16**, 1980 (1972)].

<sup>2</sup>M. Brambilla, Nucl. Fusion **16**, 47 (1976).

<sup>3</sup>M. Porkolab, Phys. Fluids **17**, 1432 (1974).

<sup>4</sup>G. J. Morales and Y. C. Lee, Phys. Rev. Lett. **35**, 930 (1975).

<sup>5</sup>G. L. Johnston, F. Y. F. Chu, C. F. F. Karney, and A. Bers, Research Laboratory of Electronics, Massachusetts Institute of Technology, Plasma Research Report PRR 76/18-2 (1976); H. H. Kuehl, Phys. Lett. A **61**, 235 (1977); C. F. F. Karney, A. Sen, and F. Y. F. Chu, Phys. Fluids **22**, 940 (1979).

<sup>6</sup>D. J. Kaup and A. C. Newell, Bull. Am. Phys. Soc. **21**, 1095 (1976); A. C. Newell, Lectures Appl. Math. **15**, 157 (1974).

<sup>7</sup>A. Bers, in *Plasma Physics - Les Houches 1972* (Gordon and Breach, New York, 1975), p. 131.

<sup>8</sup>C. Daughney, Nucl. Fusion **15**, 967 (1975).

<sup>9</sup>V. E. Zakharov and A. Shabat, Zh. Eksp. Teor. Fiz. **61**, 118 (1971) [Sov. Phys.-JETP **34**, 62 (1972)].

<sup>10</sup>F. W. Chambers and A. Bers, Phys. Fluids **20**, 466 (1977);

- V. Fuchs and G. Beaudry, *ibid.* **21**, 180 (1978).
- <sup>11</sup>A. H. Reiman, A. Bers, and D. J. Kaup, *Phys. Rev. Lett.* **39**, 245 (1977); and **39**, 850 (1977); A. H. Reiman, *Phys. Fluids* **21**, 1000 (1972).
- <sup>12</sup>M. J. Ablowitz, D. J. Kaup, A. C. Newell, and H. Segur, *Stud. Appl. Math.* **53**, 249 (1974); J. Satsuma and N. Yajima, *Prog. Theor. Phys. Suppl.* **55**, 284 (1974).
- <sup>13</sup>N. R. Pereira (private communication).
- <sup>14</sup>S. V. Mankov, *Zh. Eksp. Teor. Fiz.* **65**, 1392 (1973) [*Sov. Phys-JETP* **38**, 693 (1974)]; H. Segur and M. J. Ablowitz, *J. Math. Phys.* **17**, 710 (1976); H. Segur, *J. Math. Phys.* **17**, 714 (1976).
- <sup>15</sup>A. Bers in *Proceedings of the Third Topical Conference on Radio Frequency Heating* (California Institute of Technology, Pasadena, Calif., 1978), p. A1-1.
- <sup>16</sup>E. Apgar, B. Coppi, A. Gondhalekar, H. Helava, D. Komm, F. Martin, B. Montgomery, D. Pappas, R. Parker, and D. Overskei, in *Plasma Physics and Controlled Nuclear Fusion Research 1976* (International Atomic Energy Agency, Vienna, 1977), Vol. 1, p. 247.
- <sup>17</sup>A. Sen, C. F. F. Karney, G. L. Johnston, and A. Bers, *Nuclear Fusion* **18**, 171 (1978).
- <sup>18</sup>H. H. Kuehl, *Phys. Fluids* **19**, 1972 (1976).
- <sup>19</sup>H. Sanuki and T. Ogino, *Phys. Fluids* **20**, 1510 (1977).